

5

CHAPTER - 5

RESULTS AND DISCUSSION

5.1 DOCUMENTATION OF RESULTS :

Results of the numerical experiments, performed in the first instance to access the effect of various key parameters and then after selecting these parameters, finally to investigate the effect of aspect ratio on free convection from rectangular enclosures, have been documented for permanent record and possible further study. These records are available in the form of supplement : 1 and supplement : 2 with the original copy of the thesis, while a representative sample of results is included in Appendix : A-7 as a ready reference.

Supplement : 1 contains outputs obtained on an 80 character dot matrix printer attached to INCONIX System 4000 computer, which may be categorised as :

- i) 5 printouts containing effect of mesh size i.e. number of elements NEL varying from 50 to 200 and mesh size from 6 x 6 to 11 x 11 matrix.
- ii) 10 printouts containing effect of tolerance levels - tolerance level varying from 0.1% to 7.5%.
- iii) 2 printouts containing the results of the sensitivity analysis.
- iv) 1 printout containing the output for 11 x 11 mesh size i.e. 200 number of elements.
- v) 2 printouts containing iterationwise output for horizontal and vertical enclosures for comparison and for studying

the cause of arithmetic overflow condition appearing prematurely with vertical enclosure.

- vi) 2 printouts containing effect of boundary condition.
- vii) 1 printout containing the output with double precision computations.
- viii) 5 printouts containing the results for various aspect ratios varying from 30 to 300.

Supplement : 2 contains outputs obtained on a 132 character line printer attached to IBM 360 computer. Though the results of this supplement are in error for Nusselt number computations, bulk of information available in the form of temperature, stream function and vorticity distributions and their contours generated by the printer, is invaluable. This supplement contains the following. :

- i) 1 printout containing effect of overrelaxation factor on conduction solution.
- ii) 5 printouts containing the results for various aspect ratios varying from 5 to 50. The results follow double precision computations, use 200 number of elements and generate temperature, stream function and vorticity contours automatically.

The results documented in Supplement : 1 were represented in Fig.5.1 to Fig.5.9 as under :

- i) Fig.5.1 shows Nu v/s Ra curve on logarithmic scale for aspect ratios varying from 1 to 300, in case of horizontal enclosures. The curve shows the appearance

of three distinct regions based on AR e.g. $1 \leq AR \leq 5$, $5 \leq AR \leq 10$ and $10 \leq AR \leq 300$. The detailed study of which continues in subsequent figures.

- ii) Fig.5.2 shows the correlations for $10 \leq AR \leq 200$ in case of horizontally oriented enclosures. It is interesting to note that this figure also indicates the presence of three distinct regions based on Ra e.g. $Ra \leq Ra_{c1}$, $Ra_{c1} \leq Ra \leq Ra_{c2}$ and $Ra \geq Ra_{c2}$.
- iii) Critical Rayleigh numbers Ra_{c1} and Ra_{c2} which divide the correlation curves into three regions, strongly depend upon aspect ratio AR. This is shown in Fig.5.3.
- iv) An attempt is made to correlate the results for $1 \leq AR \leq 5$ in Fig.5.4, however, the scatter of the data points indicates the need for further research in this region.
- v) Fig.5.5 represents the effect of enclosure inclination θ in the first quadrant ($\theta \leq 90^\circ$), on gap Nusselt number Nu. A definite instability is observed at $\theta > 5^\circ$ for higher Ra values at all aspect ratios.
- vi) Fig.5.6 and Fig.5.7 represent the effect of enclosure inclination in first quadrant ($\theta \leq 90^\circ$) on gap conductance h , with aspect ratio AR as a parameter. These figures show that a definite conclusion can not be drawn because of the instability.
- vii) Logarithmic plot of Nu v/s Ra relationship for various enclosure inclinations in the second quadrant ($90^\circ \leq \theta \leq 180^\circ$) is shown in Fig.5.8 for a particular aspect ratio. Well behaved curves indicate stability and a possibility of obtaining a correlation in this range

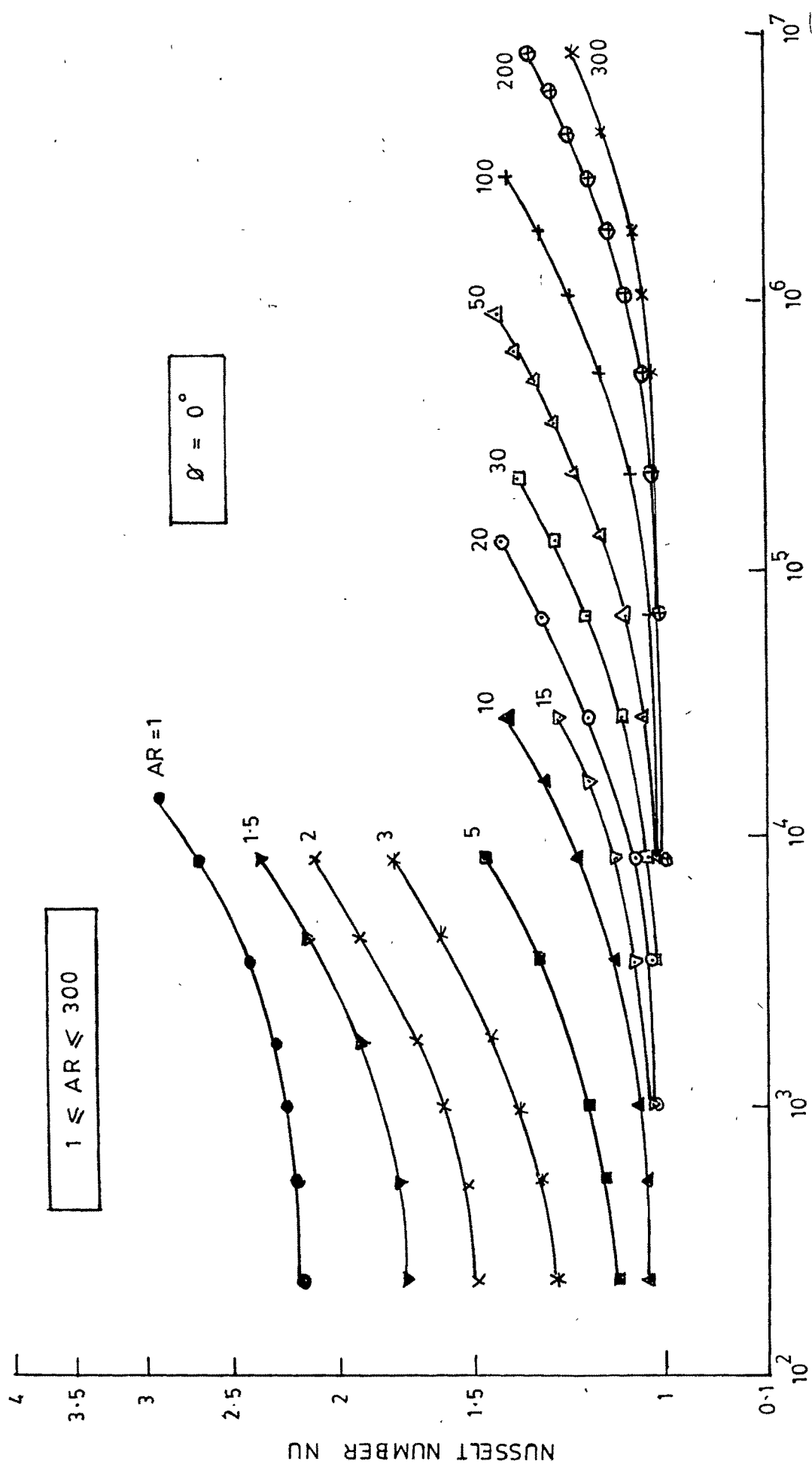
of inclinations, if a study is pursued further for various aspect ratios.

- viii) An interesting comparison is made at $\theta = 180^\circ$ where the enclosure is heated from above, for two widely different aspect ratios, in Fig.5.25 indicating a departure from classical conduction behaviour, at high Ra values for low aspect ratio enclosures. A study for low aspect ratio regions ($AR \leq 20$) at high Rayleigh numbers, if pursued, would definitely result in revealing observations.

5.2 DISCUSSION OF RESULTS :

Findings of the present investigation are summarised in the preceding article, which also include various plots in Fig.5.1 to Fig.5.27 for better understanding of the problem.

As is evident from Fig.5.1, three distinct convection regimes can be identified, based on aspect ratio. For aspect ratios between 10 and 300, Nu v/s Ra curves tend to merge into a single horizontal line of $Nu \approx 1$ as Ra decreases. This shows that heat transfer essentially takes place by conduction in the beginning, till a certain Rayleigh number is exceeded. This Rayleigh number can be called first critical Rayleigh number Ra_{c1} , as a second criticality also appears later, in these curves. This confirms with the well known classical observation made by Silveston²³. However, Silveston experimented with cylindrical enclosures, who observed only one criticality of the type just mentioned and he observed that the critical Rayleigh number is 1700 ± 51 , a value that is independent of aspect ratio. Present results contradicts this second observation as it was observed that Ra_{c1} is strongly dependent upon aspect ratio. Fig.5.3 indicates this very clearly



RAYLEIGH NUMBER Ra

FIG: 5.1

and the findings may be correlated as :

$$Ra_{c1} = 10 AR^2 \quad \dots \quad (5.1)$$

Onset of convection occurs the moment the Rayleigh number exceeds Ra_{c1} , as Nu v/s Ra curve starts rising from a constant value of $Nu \approx 1$. This is clear from Fig.5.1. This convection is of cellular character, as it is a weak function of Rayleigh number. This can be observed in Fig.5.2 also, where the curves at different aspect ratios merge into a single slanting line representing $Nu \cdot AR^{0.125}$ v/s Ra relationship. This behaviour of cellular convection can be correlated as :

$$Nu = 0.8463 Ra^{0.0675} AR^{-0.125} \quad \dots \quad (5.2)$$

for $Ra_{c1} \leq Ra \leq Ra_{c2}$

Above correlation clearly indicates that the heat transfer in cellular convection is dependent upon aspect ratio AR in addition to Rayleigh number Ra and also that heat transfer reduces with increase in aspect ratio.

Fig.5.2 reveals that the curves, starting horizontally, subsequently merge into a single slanting line at a first critical Rayleigh number Ra_{c1} , however, finally they end into separate parallel lines with an increased slope at another critical Rayleigh number, called second critical Rayleigh number Ra_{c2} .

These parallel lines at $Ra \geq Ra_{c2}$ can be correlated by:

$$Nu = 0.6760 Ra^{0.125} \cdot AR^{-0.25} \quad \dots \quad (5.3)$$

for $Ra \geq Ra_{c2}$

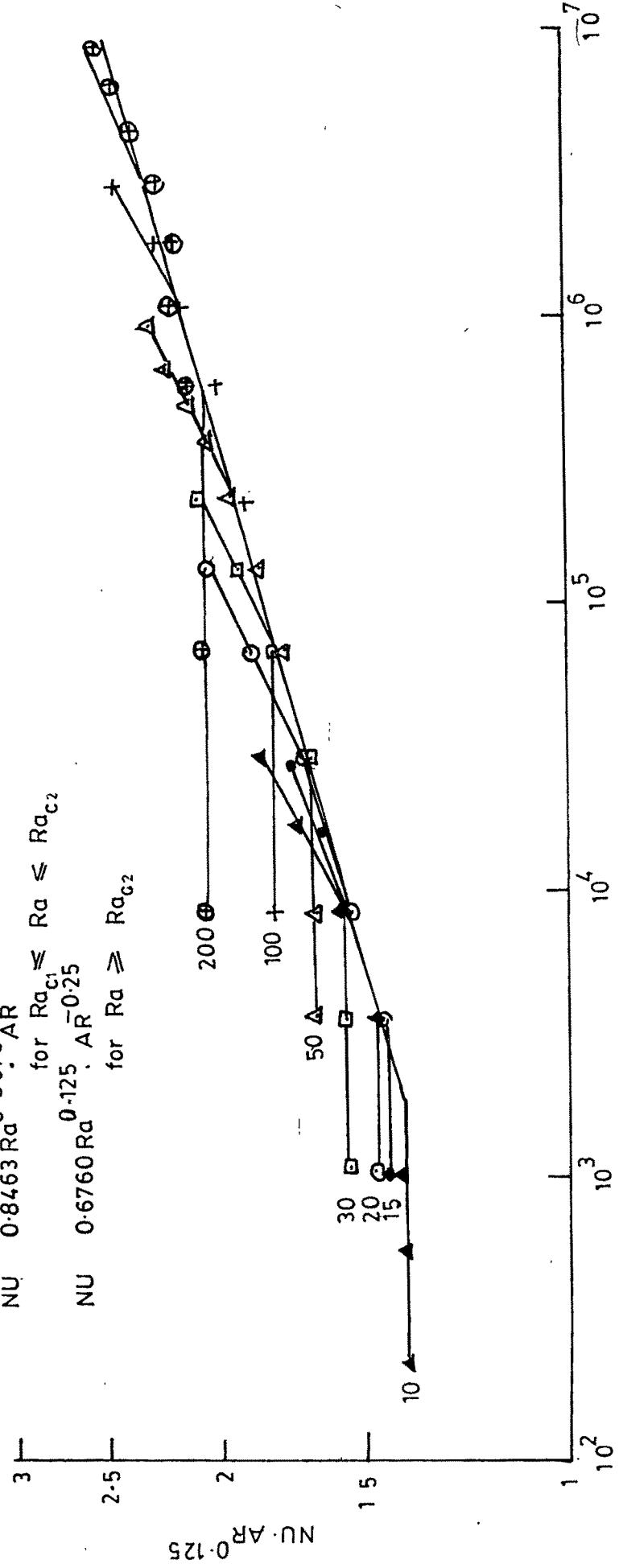
Above correlation clearly indicates the appearance of convective boundary layer flow in the enclosure due to an introduction of $Ra^{0.125}$ factor.

$\phi = 0^\circ$

$10 \leq AR \leq 200$

- ▲ AR = 10
- AR = 20
- △ AR = 50
- ⊕ AR = 200
- AR = 15
- ◻ AR = 30
- + AR = 100

$NU = 1$ for $Ra \leq Ra_{c1}$
 $NU = 0.8463 Ra^{0.0675} AR^{-0.125}$ for $Ra_{c1} \leq Ra \leq Ra_{c2}$
 $NU = 0.6760 Ra^{0.125} AR^{-0.25}$ for $Ra \geq Ra_{c2}$



Ra

FIG: 5.2

Onset of boundary layer convection occurs when Ra exceeds Ra_{c2} , as is also evident from Fig.5.3 and is given by :

$$Ra_{c2} = 70 AR^2 \dots (5.4)$$

Thus, our findings for $10 \leq AR \leq 300$ may be summarised as under :

Heat transfer in horizontal enclosures is essentially by conduction until Ra value exceeds the first critical Rayleigh number, when onset of cellular convection occurs. On further increasing Rayleigh number, cellular convection may turn into boundary layer convection, if it exceeds the second critical Rayleigh number. Both the critical Rayleigh numbers are strongly dependent upon AR while heat transfer in both cellular and boundary layer convection also depends upon aspect ratio.

As is evident from Fig.5.3, onset of both cellular and boundary layer convection is delayed with increase in aspect ratio. This may be explained by considering the mechanism of heat transfer in enclosures. Heat transfer in enclosures may be thought of due to three distinct mechanisms. Pure conduction from hotter lower surface to cooler upper surface is evidently the primary mechanism while buoyancy driven convection between horizontal surfaces is the secondary mechanism and is due to adverse temperature gradients in vertical direction. There appears also a secondary convection due to horizontal temperature gradients resulting from an interaction of side walls. It may be noted that it is this interaction of side walls, in addition to adverse vertical temperature gradients, that brings about onset of cellular and boundary layer convection. It is this last mechanism which is responsible for delaying the onsets of these convective flows, with increase in aspect ratio. These mechanisms, in different context, are described

$10 \leq AR \leq 200$

$\phi = 0^\circ$

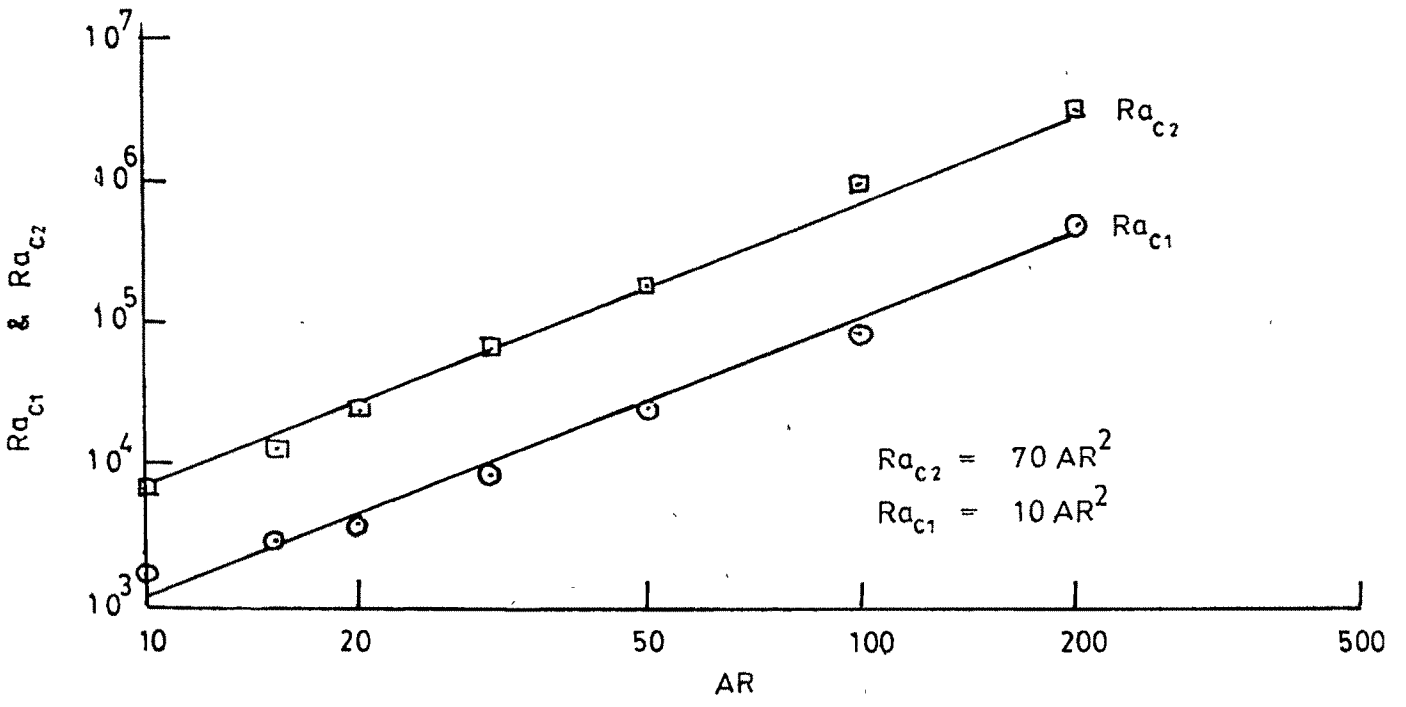


FIG: 5-3

elsewhere by Zhong et al⁶⁸.

The other two regimes based on aspect ratio e.g. $1 \leq AR \leq 5$ regime where an attempt is made to obtain a correlation (Fig.5.4) and $5 \leq AR \leq 10$ regime where no such attempt was made, requires carefully planned research effort, before any definite conclusions can be drawn. Linthorst et al's⁵⁸ LDA study and flow visualisation experiments in this regime is of particular mention here.

Fig.5.5, 5.6 and 5.7 represent effect of enclosure orientation on heat transfer for $0^\circ \leq \theta \leq 90^\circ$. It is difficult to draw any definite conclusions from these figures. It may be noted, however, that the curves in the region $0^\circ \leq \theta \leq 5^\circ$ behave normally as anticipated, while they show a noticeable departure in the region $15^\circ \leq \theta \leq 90^\circ$. It is also observed that heat transfer is minimum for AR between 30 to 60 at a gap height of 10 mm and for AR between 60 to 80 at a gap height of 20 mm, at all the inclinations studied. On the whole, however, it is necessary to reformulate the problem in this range of inclination, due to uncharacteristic nature of the curves. This uncharacteristic behaviour of the fluid may be attributed to invalidity of some of the assumptions made in the present analysis, like Boussinesq approximation, constant properties approximation, two-dimensional approximation etc. It may be noted that Zhong et al⁶⁸ realised this and removed Boussinesq approximation and constant properties approximation from their analysis. They, however, could not get rid of haphazardness of results in the region $0^\circ \leq \theta \leq 90^\circ$, and attributed this to the two-dimensional approximation which was not removed.

Well behaved curves were obtained in Fig.5.8 for enclosure orientations in the second quadrant e.g. $90^\circ \leq \theta \leq 180^\circ$ for an aspect ratio of 20. This suggests the possibility of obtaining a correlation if a study is pursued further.

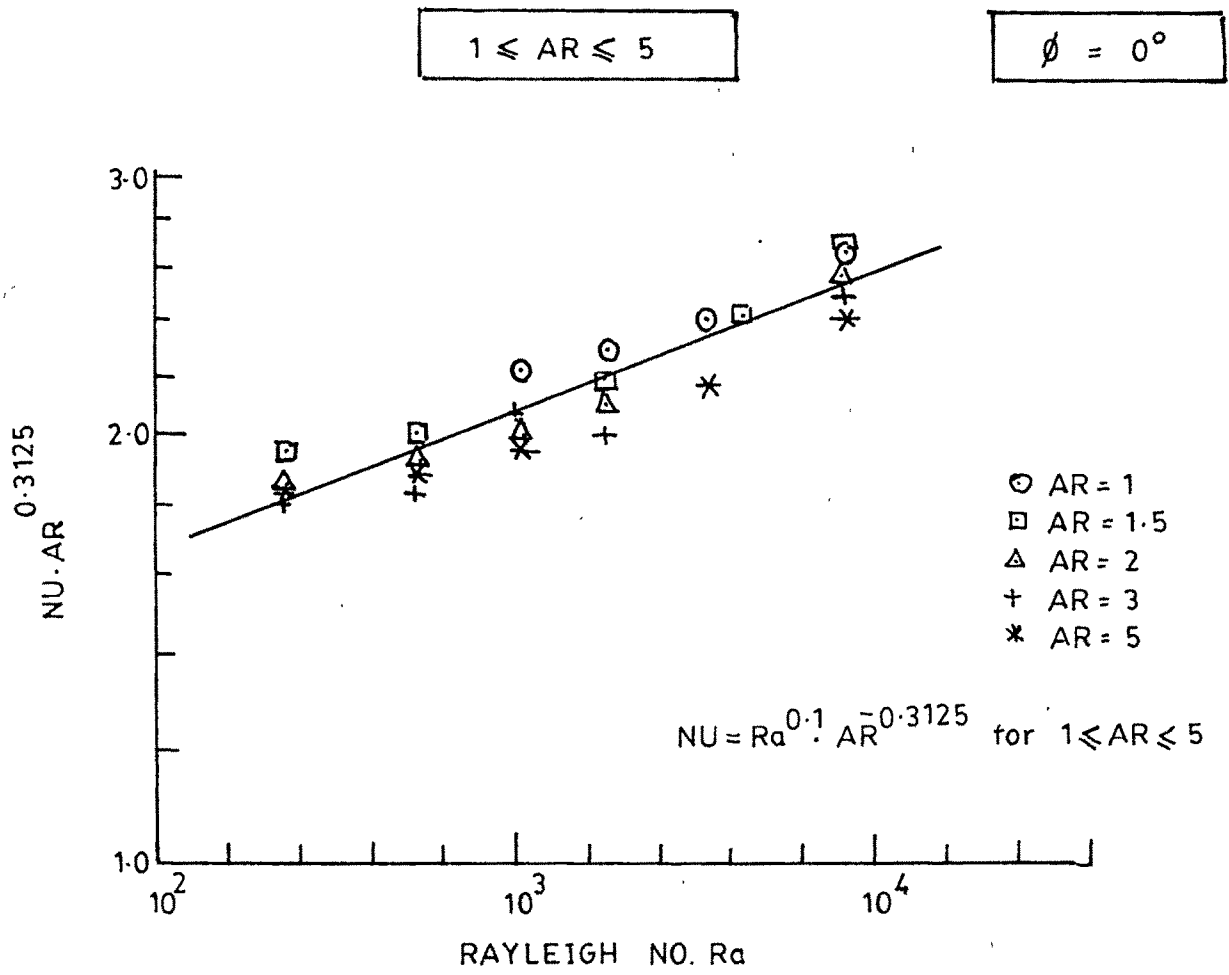
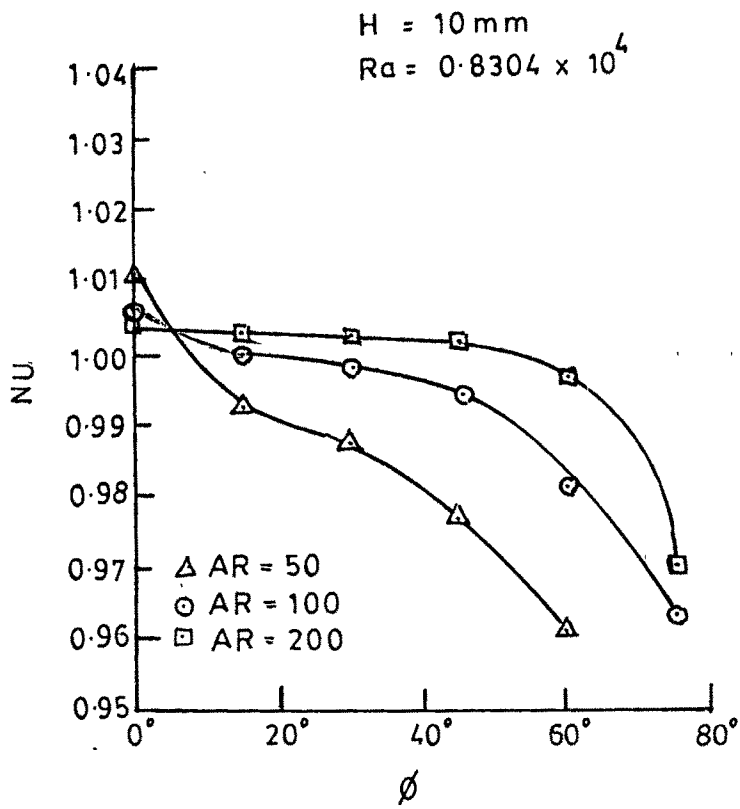
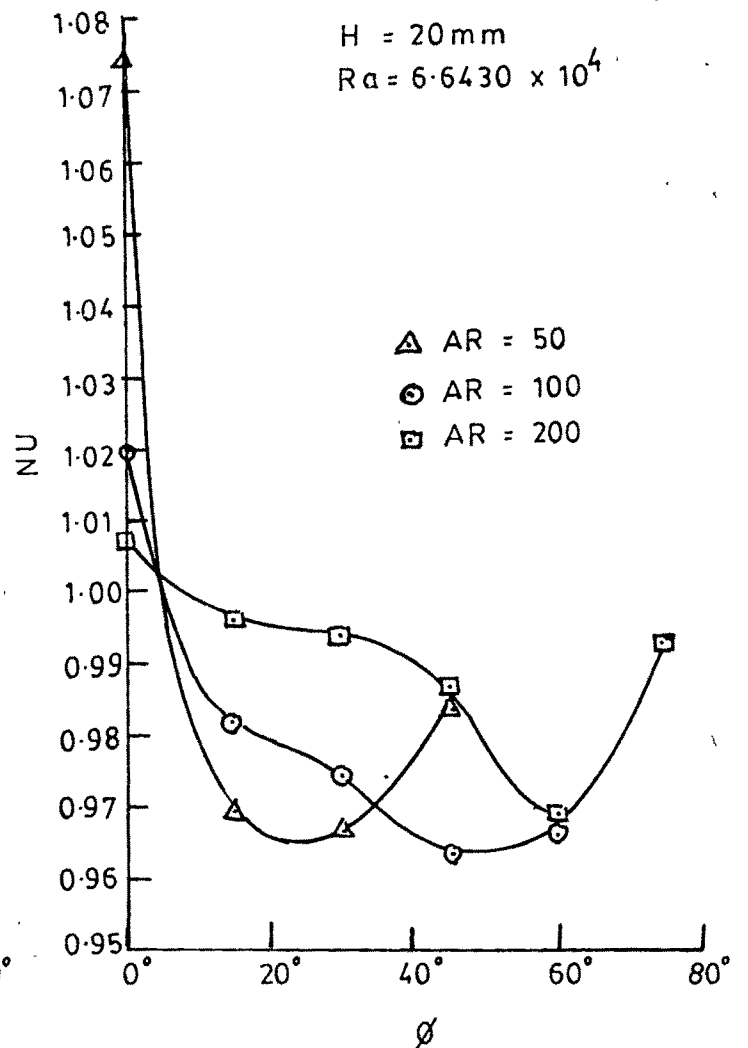


FIG: 5-4



(a)



(b)

FIG: 5.5

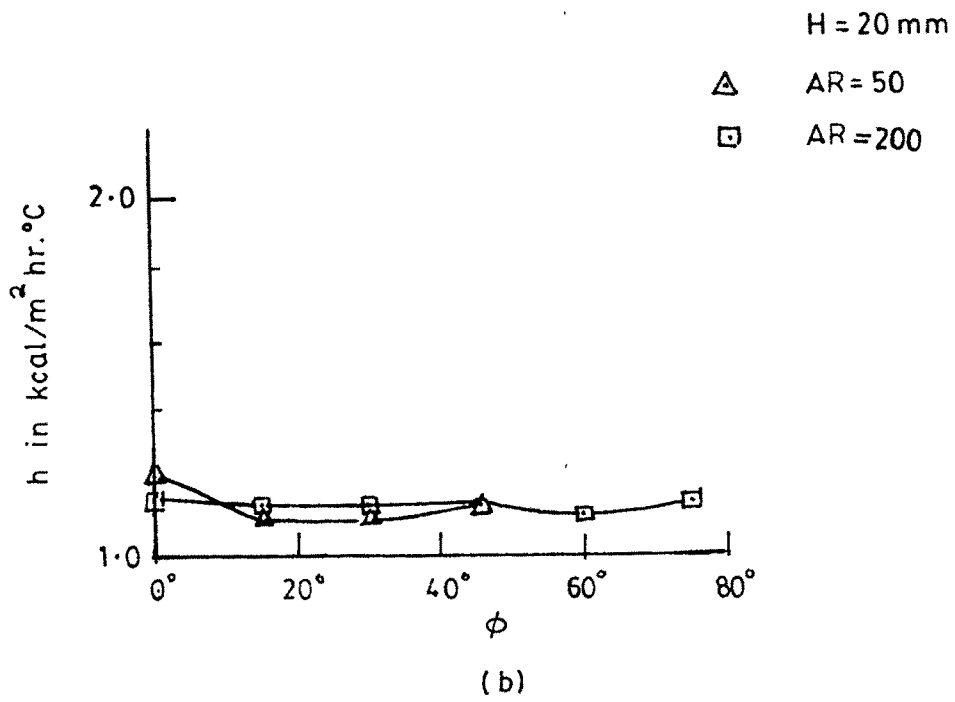
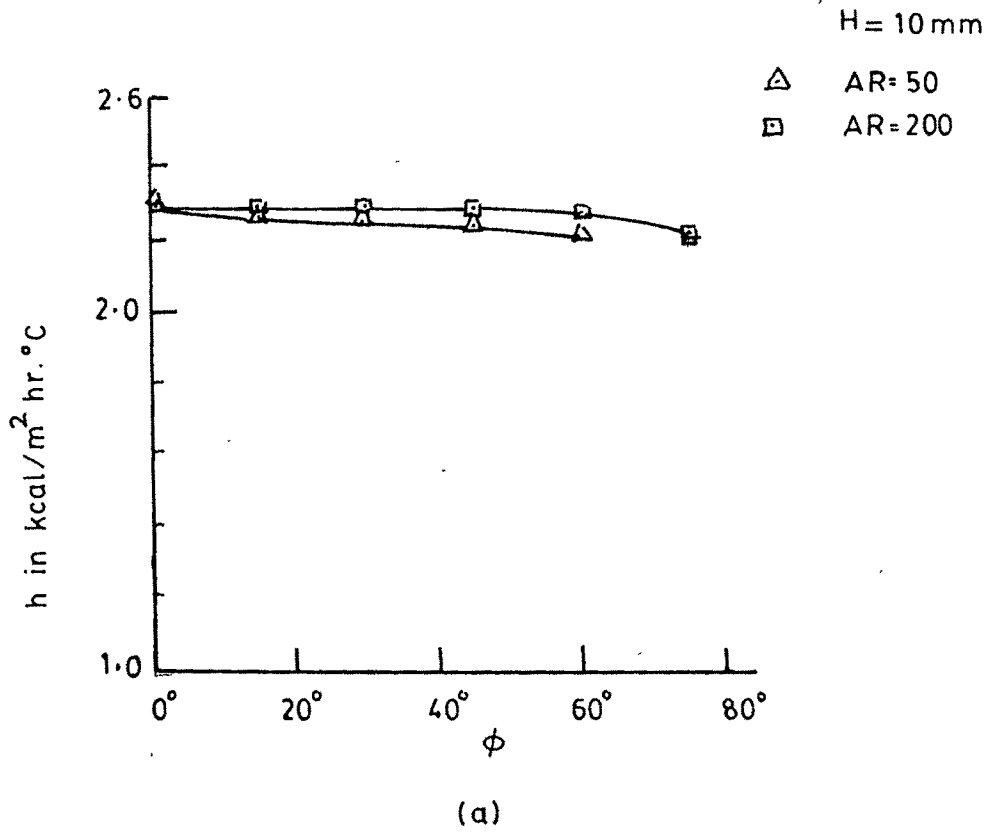


FIG: 5.6

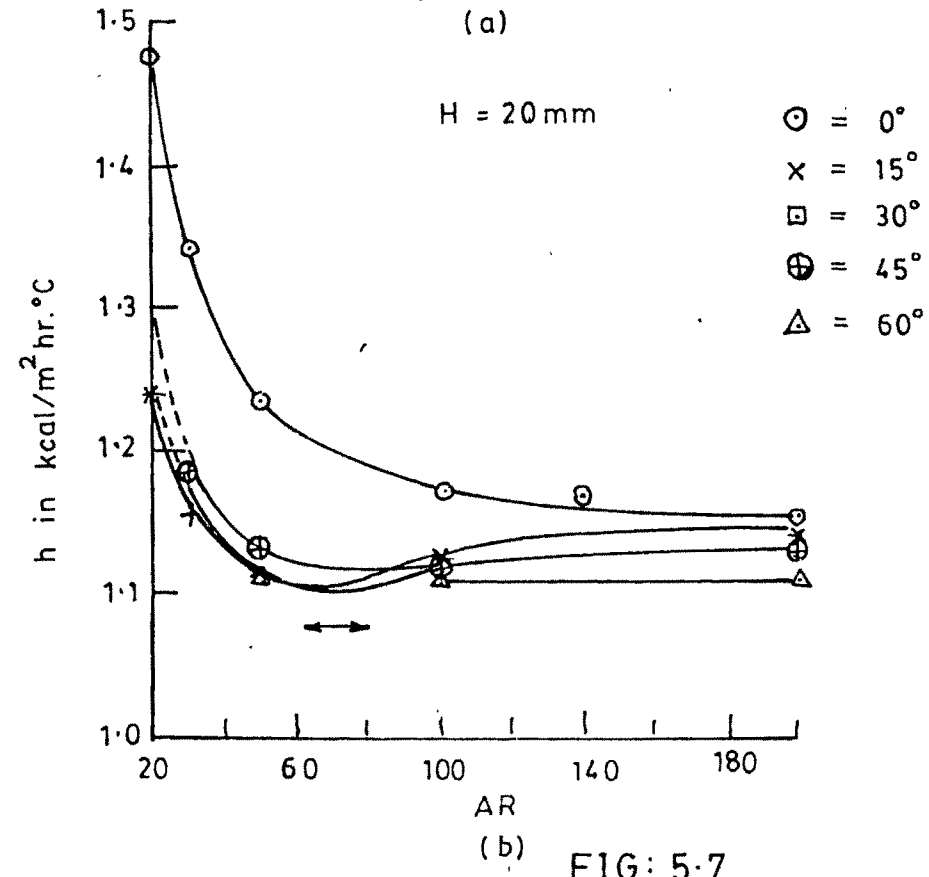
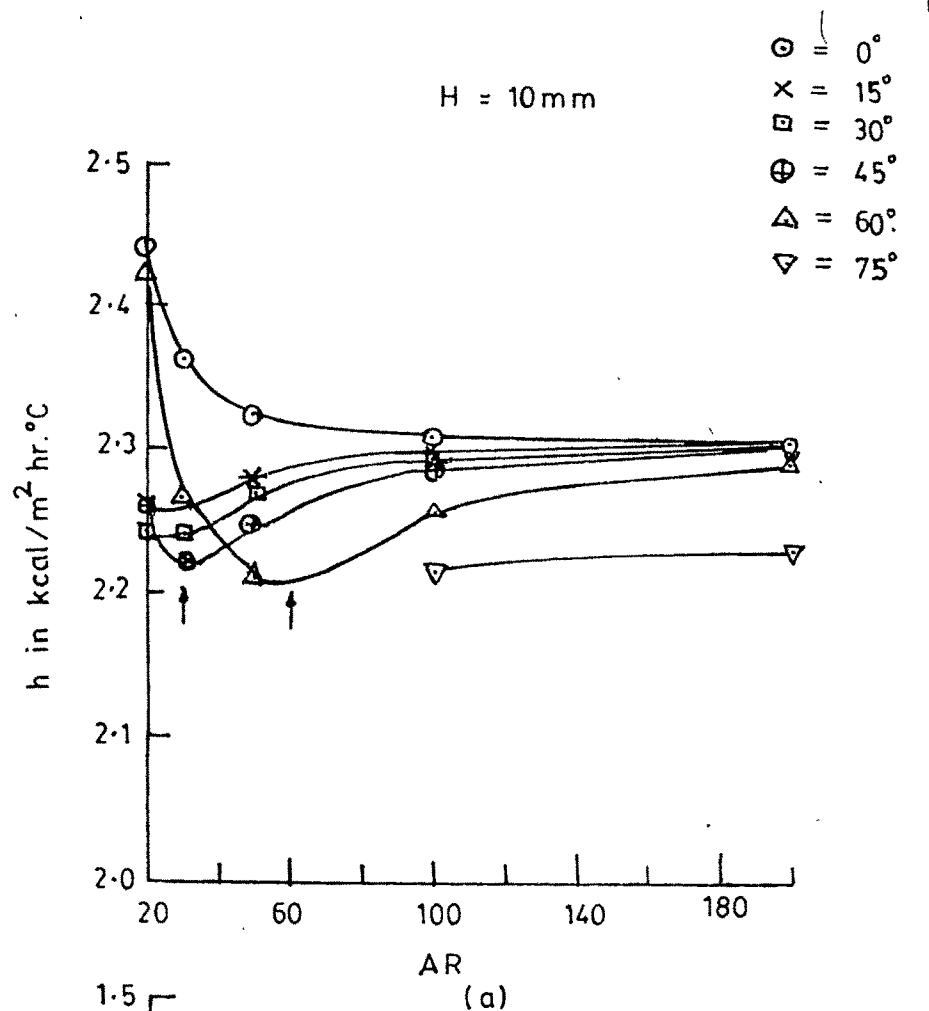


FIG: 5.7

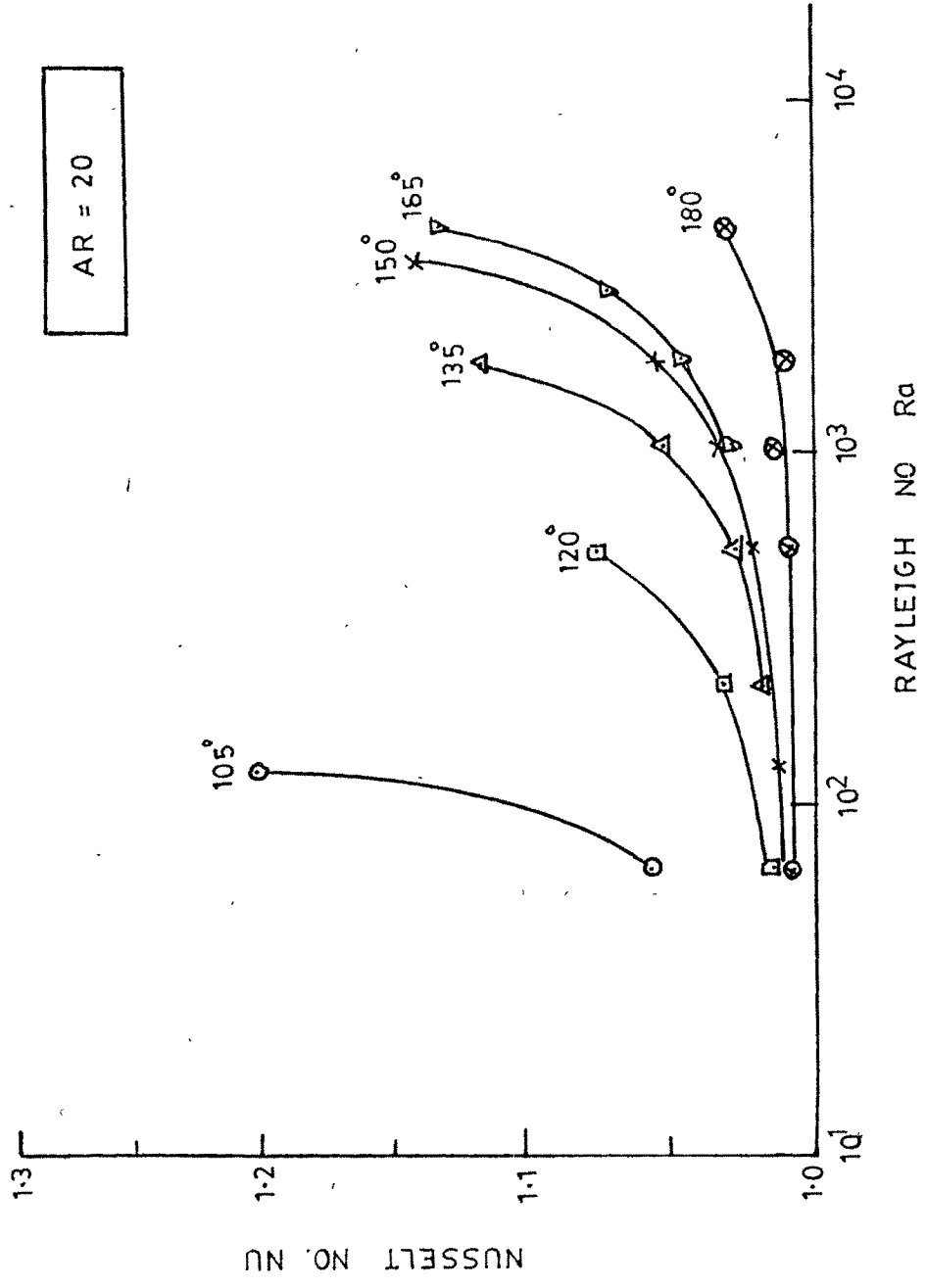


FIG: 5.8

A detailed survey of existing literature on numerical and experimental study of the effect of the orientation on free convection in rectangular enclosures, at this juncture, is not out of place, as it may help in drawing a comparison between our results and those of earlier investigators.

Strada and Heinrich⁶⁰ reported in 1982, the results of the numerical experiments on steady, laminar free convection in rectangular cavities for Rayleigh numbers of upto 10^7 , angle of inclination varying from 0° to 180° with reference to horizontal and aspect ratios of 1, 5 and 10. They used a penalty function finite element algorithm with primitive fluid variables in their study.

As was reported by them, vertical enclosures have been widely investigated by numerical methods, however, for other inclinations, a few numerical studies have been reported in literature. Numerical results for inclined cavities using Galerkin method and using finite difference schemes were reported earlier, while they used penalty function approach for obtaining a solution.

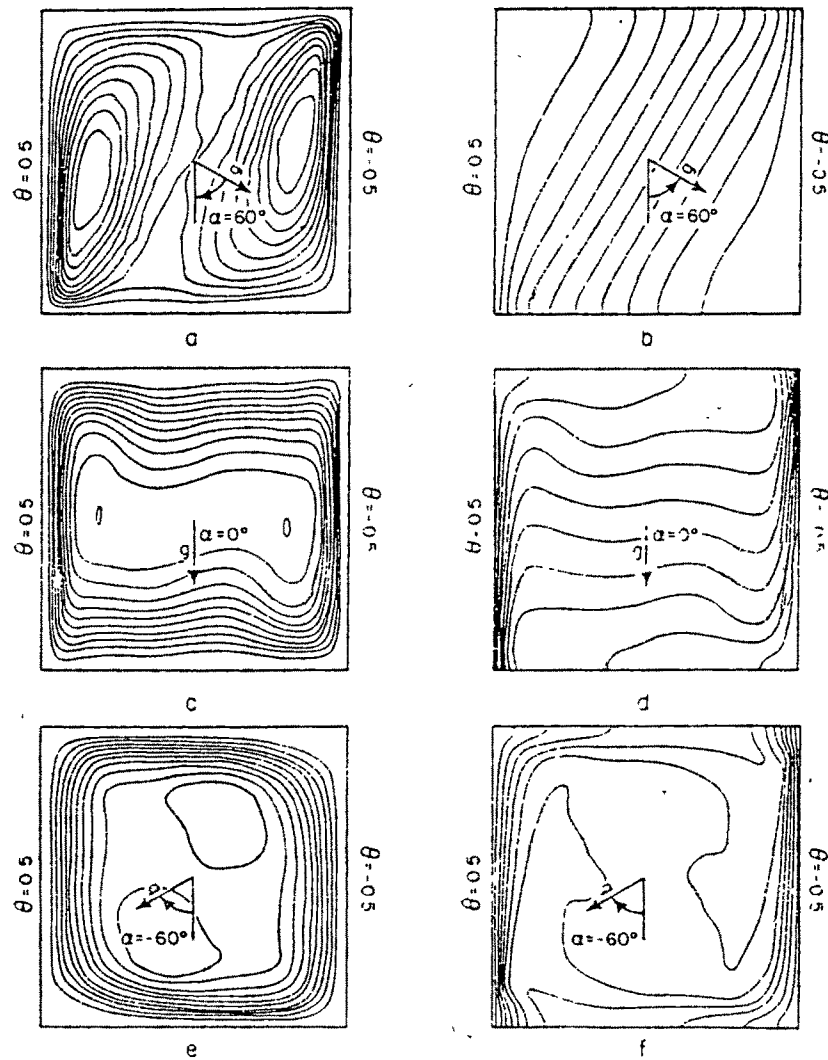
Boussinesq approximation was used for obtaining the basic equations which were non-dimensionalised before discretizing using the penalty function finite element method. The penalty parameter λ was chosen as 10^9 for Ra upto 10^5 and as 10^{10} for higher Ra values. The Prandtl number was assumed as 1.0 for AR = 1 and as 1.43 for AR = 5 and 10. Nine noded, bi-quadratic, Lagrangian elements in a non-uniform mesh, different for different aspects ratios, were used, following Gill's suggestion and after numerical experimentation for their selection.

They found that with increase in Rayleigh number, more refinement is needed to reach a converged solution, resulting in a significant increase in the computational cost at high Ra values for high aspect ratio enclosures. They obtained excellent agreement with the results of earlier investigators at low Ra values for vertical, square cavities and hence assumed the adequacy of their analytical model.

They observed, particularly at higher Ra values (from 10^5 to 10^7) that they could not obtain the solutions for enclosure orientations in the region of 0° to 25° and 155° to 180° with reference to horizontal. This, they believed, was due to physically different mode of circulation occurring in this range of inclinations, that is not picked up by the numerical model, used by them.

Fig.5.9 shows the stream function and temperature contours for a square enclosure (AR=1) at Ra value of 10^6 , for various orientations, obtained by them. It depicts an appearance of pure boundary layer flow for vertical enclosures ($\alpha = 0^\circ$), due to gathering of all isotherms near vertical boundaries. However, at inclinations in first quadrant, for example, at $\alpha = 60^\circ$ (i.e. 30° with reference to horizontal), the isotherms reveal a cellular character of free convection in the enclosure.

The isotherms at $\alpha = -60^\circ$ (i.e. 150° with reference to horizontal) reveal an interesting pattern. They show a trend towards spreading of boundary layer isotherms in the direction of the central core region, which may, eventually at 180° inclination with reference to horizontal, result into uniformly spreaded isotherms from top to bottom in the enclosure, a characteristic pattern of conduction isotherms. Such an obvious pattern, however, was not obtained by the investigators, due to the limitation of their algorithm.



Stream function and isotherm plots for $Ra = 10^5$ and aspect ratio $A = 1$. All isotherm contours are for intervals $\Delta\theta = 0.09$. (a) Stream function for $\alpha = 60^\circ$, contours at $\psi = 0.25, 0.49, 0.74, 0.98, 1.23, 1.47, 1.72, 1.96, 2.21, \text{ and } 2.45$. (b) Isotherms for $\alpha = 60^\circ$. (c) Stream function for $\alpha = 0^\circ$, contours at $\psi = 1.54, 3.09, 4.63, 6.17, 7.72, 9.26, 10.81, 12.35, 13.89, 15.44, \text{ and } 17.0$. (d) Isotherms for $\alpha = 0^\circ$. (e) Stream function for $\alpha = -60^\circ$, contours at $\psi = 3.80, 7.60, 11.41, 15.21, 19.01, 22.81, 26.62, 30.42, 34.22, \text{ and } 38.02$. (f) Isotherms for $\alpha = -60^\circ$.

FIG: 5-9

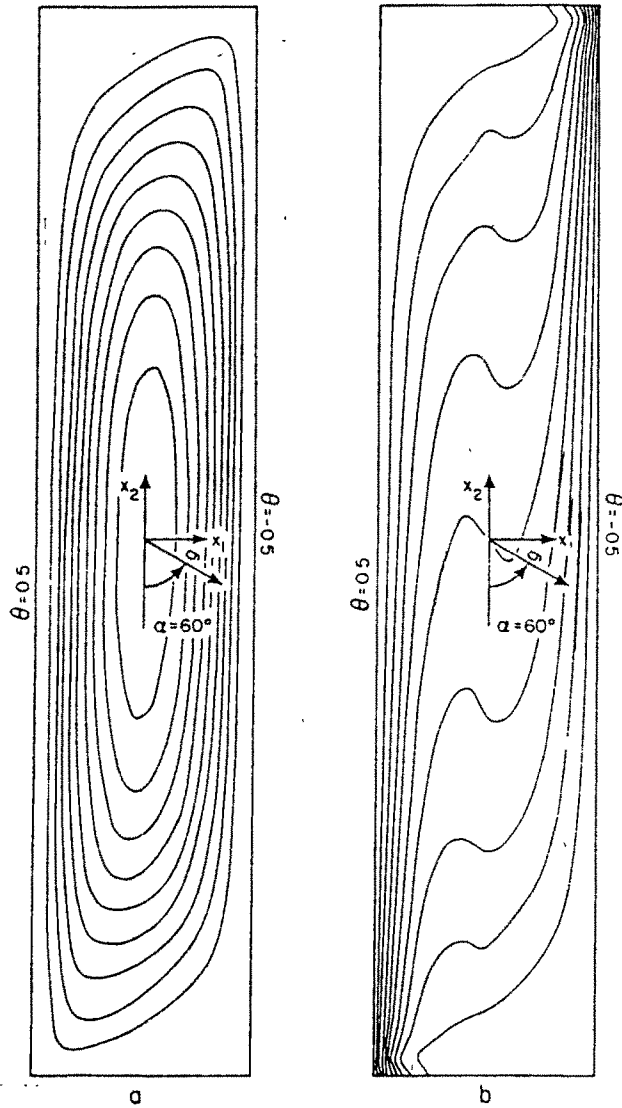
Effect of increasing aspect ratio on stream function and temperature contours, for inclinations in first quadrant and also in second quadrant, can be ascertained by comparing Fig.5.10 and 5.11 with Fig.5.9. It is apparent that increase in aspect ratio results in free convection that is conduction dominated, for both the cases of enclosure orientations, possibly due to receding effect of side walls, on free convection circulations.

Prasad and Kulacki⁶⁴ in 1984, studied the effect of aspect ratio on flow structure and heat transfer in a vertically oriented rectangular cavity, by using a numerical finite difference technique developed earlier by Gosman et al⁶⁵. They used non-uniform grids with finer grids near the walls in both the directions for Ra values greater than 200. A point iterative scheme with overrelaxation of temperature for low Ra values and under relaxation of stream function for high Ra values, was employed to solve the system of algebraic equations appropriate to the problem.

Though Prasad and Kulacki did not vary enclosure inclination in their study, their discussion about various flow regimes and their aspect ratio dependency is interesting and worth noting.

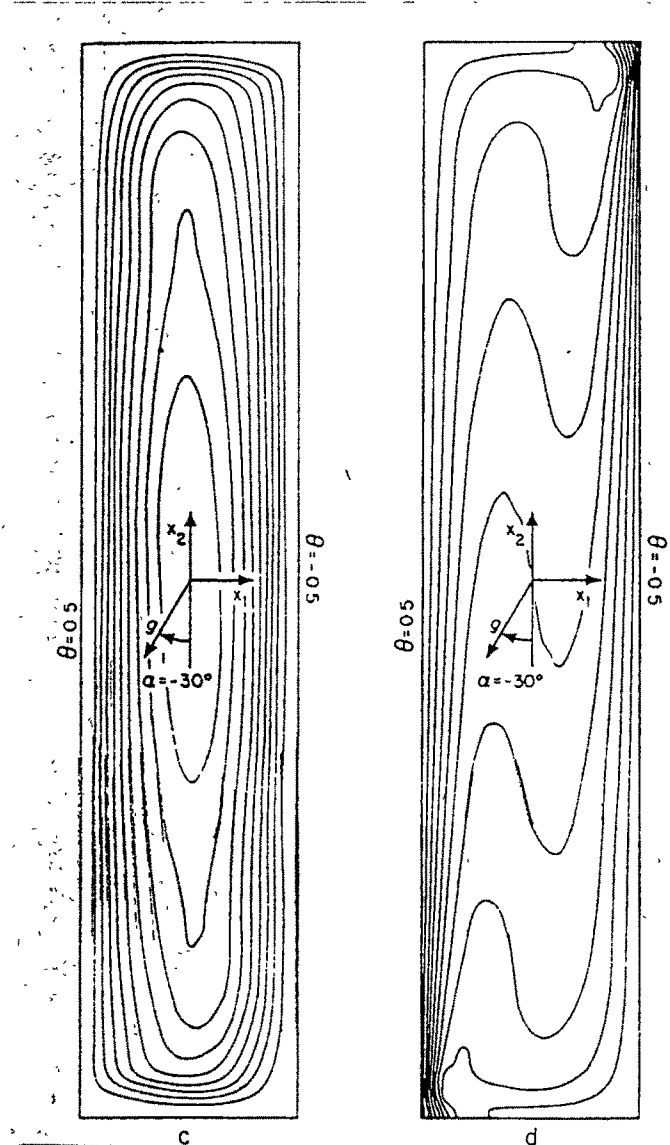
As can be observed from Fig.5.12, for any Ra value greater than 60 (based on distance between insulated surfaces), changing aspect ratio from very low value (0.01) to very high value (100) results in gradual transition from one flow regime to another in the following order :

- i) Pure conduction regime : Here, heat flows from hot surface to cold surface, strictly by conduction where the trapped fluid in the enclosure is stationary and the Nusselt number in such a case being unity.



Stream function and isotherm plots for $Ra = 1.43 \times 10^5$, $Pr = 1.43$, and aspect ratio $A = 10$. (a) Stream function values for $\alpha = 60^\circ$; contours at $\psi = 3.6, 7.2, 10.8, 14.4, 18.0, 21.6, 25.2, 28.8$, and 32.4 . (b) Isotherms for $\alpha = 60^\circ$ at intervals $\Delta\theta = 0.1$.

FIG: 5-10



Stream function and isotherm plots for $Ra = 1.43 \times 10^4$, $Pr = 1.43$, and aspect ratio $A = 10$ (Continued). (c) Stream function values for $\alpha = -30^\circ$; contours at $\psi = 5.1, 10.3, 15.4, 20.6, 30.9, 36.0, 41.1,$ and 46.3 . (d) Isotherms for $\alpha = -30^\circ$ at intervals $\Delta\theta = 0.1$.

FIG: 5-11

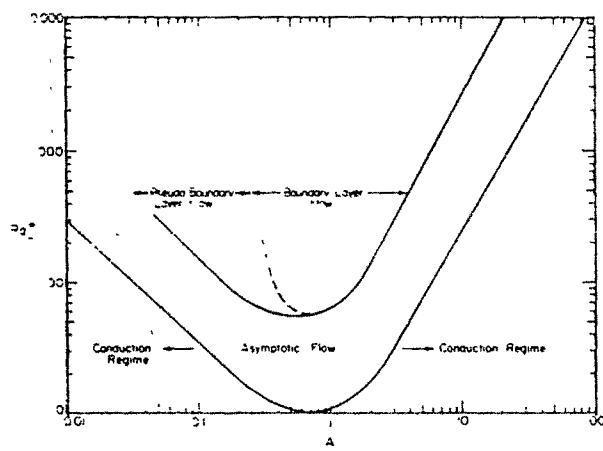


FIG: 5-12

- ii) Conduction flow regime : Moderate circulatory flow parallel to surfaces is observed, however, the central core of the fluid remains undisturbed, within which, heat flows by pure conduction. Nu increases slightly due to wall-attached circulatory flow in this regime.
- iii) Asymptotic flow regime : This regime is characterised by the stratification of the fluid in the core, in addition to increased pace of convection currents near the walls. The flow is, still however, conduction dominated.
- iv) Pseudo boundary layer flow regime : Here, the circulatory convection currents near the walls form a boundary layer flow, mainly due to stratification of the core fluid. This results in convective heat flow through the boundary layers near the walls and conductive heat flow within the central stratified core, both being of comparable magnitude.
- v) Boundary layer flow regime : In this regime, heat transfer is convection dominated and the stratified central core begins participating in heat exchange by convection.
- vi) Asymptotic flow regime : This regime reappears as aspect ratio is increased still further.
- vii) Conduction flow regime : Reappearance of this regime shows that heat transfer starts becoming conduction dominated as aspect ratio is increased further.
- viii) Pure conduction regime : This reappears at very high values of aspect ratios, where the side walls

that initiate and propagate circulatory flows, are far away and fail to initiate such flows, resulting in heat transfer by pure conduction in this regime.

Zhong et al⁶⁸ in 1985, obtained the effect of enclosure orientation on free convection from square enclosures, using a finite difference technique. They used temperature dependent transport properties for the trapped fluid and ideal gas equation of state instead of the classical and customary Boussinesq approximation, in their study. The governing partial differential equations were normalized before discretization, which ~~are~~ suitable for finite differencing.

They obtained the isotherms and stream function contours at various inclinations, as shown in Fig.5.13. Their results are comparable to those obtained by Strada and Heinrich, discussed earlier.

In an attempt to obtain a correlation for including the effect of enclosure inclination, they developed a correlation function $K_\psi = 2/\pi \psi \sin\psi$ where ψ is an inclination of colder surface with reference to horizontal and K_ψ is defined by :

$$K_\psi = (Nu - Nu_{0^\circ}) / (Nu_{90^\circ} - Nu_{0^\circ})$$

Fig.5.14 and 5.15 represent this function as a function of enclosure inclination. It is clear from these figures, that the correlation function fits excellently with their numerical results and the results of earlier experiments done by other investigators, in the second quadrant, where conduction dominated heat transfer is expected due to bottom heavy arrangement of the trapped fluid in the enclosure. However, the results fail to fit into any correlation function in the first quadrant, where top heavy arrangement of the trapped fluid in the

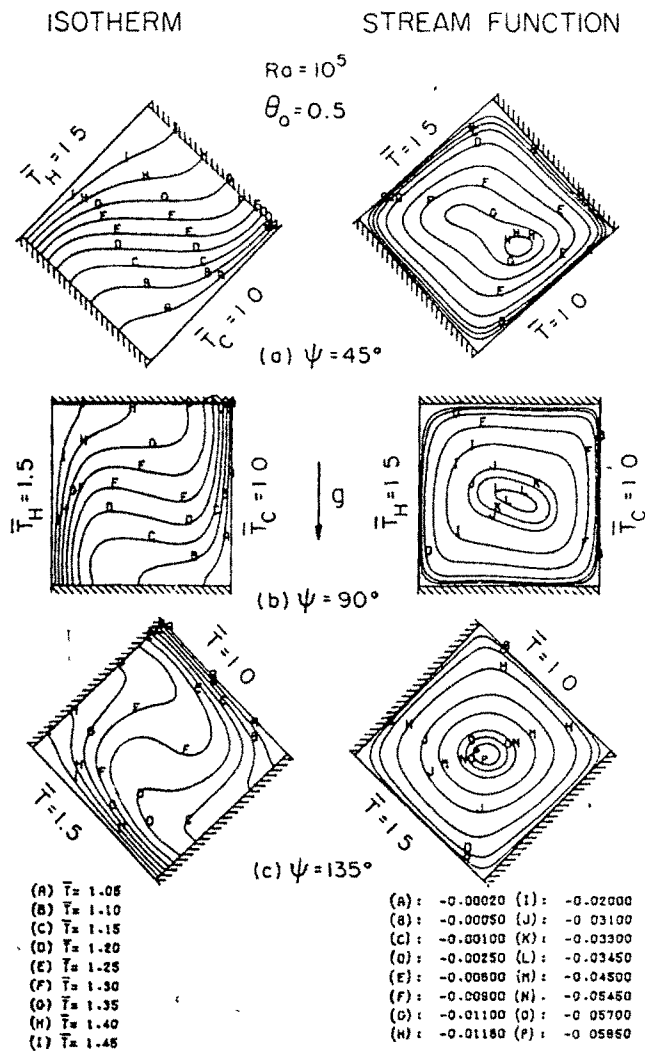


FIG: 5-13

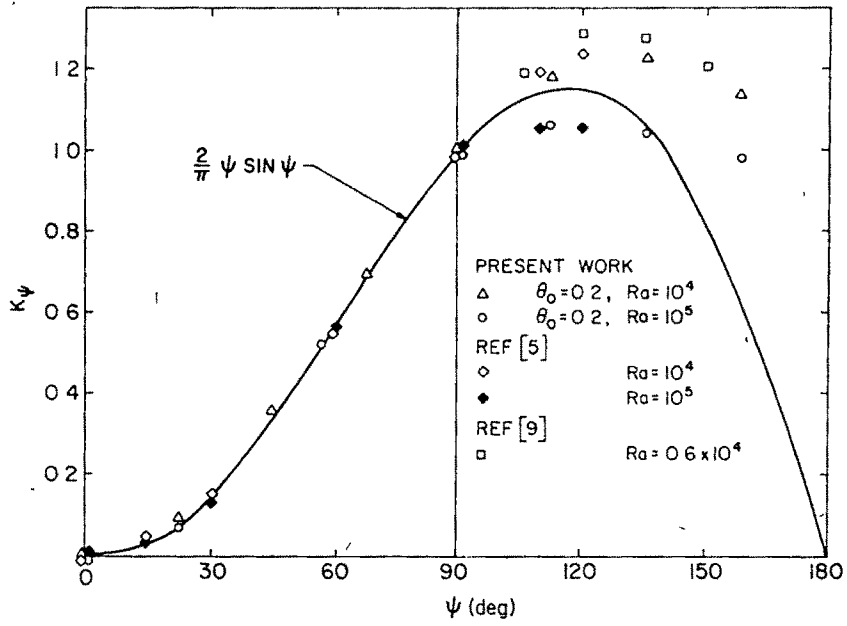


FIG: 5-14

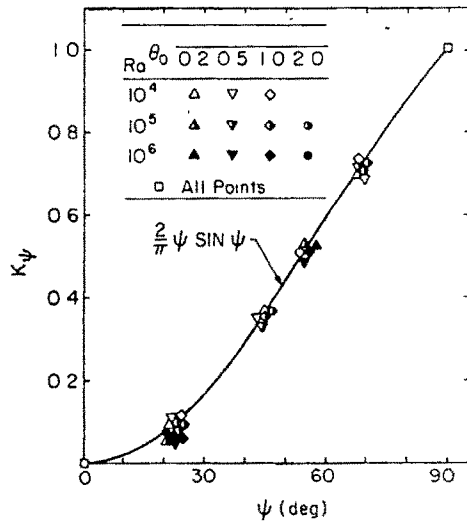


FIG: 5-15

inclined enclosure, is supposed to make the flow unstable, consisting of multiple cells rolling three-dimensionally along an incline. It is also interesting to note that their algorithm failed to provide any solution for horizontal enclosures, heated from below. Zhong et al failed to provide any explanation for such an anomaly in their results except that they attributed this to unstable temperature gradients, complicating the flow and temperature fields, resulting in instability.

Flow visualisation study using smoke injection and Laser Doppler Anemometer measurements of fluid velocities, for natural convection in inclined air-filled enclosures, were made by Linthorst et al⁵⁸ in 1981. They varied aspect ratio from 0.25 to 7, inclination from 0° to 90° and Rayleigh number from 5×10^3 to 2.5×10^5 . Fig.5.16, 5.17 and 5.18 represent flow pictures for vertical, horizontal and inclined orientations, respectively.

They observed secondary and tertiary motion in vertical enclosures at $AR \geq 1$ and $Ra > 1.4 \times 10^5$, while in horizontal enclosures, longitudinal rolls were observed for $AR \leq 1$. For $AR > 1$, toruslike flow patterns were visualised for horizontal enclosures.

Increasing angle of inclination of the enclosure with reference to horizontal and Rayleigh number, results in the transition of stationary flow into non-stationary flow and of two-dimensional flow into three-dimensional flow. It was also observed that with decreasing aspect ratio, the flow remains stationary for higher Rayleigh numbers and smaller inclinations.

LDA measurements showed that increase in Ra values results in the development of a boundary layer flow while decrease in inclination ϕ results in disappearance of boundary layer flow and appearance of cellular flow due to increased velocities in the core region.

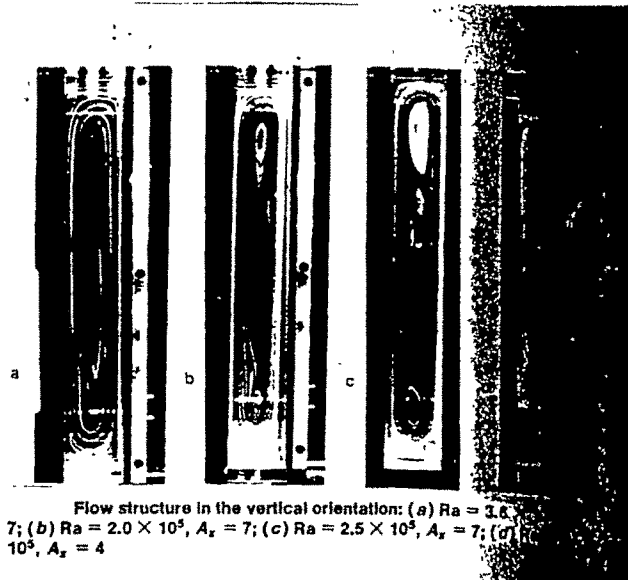


FIG: 5-16

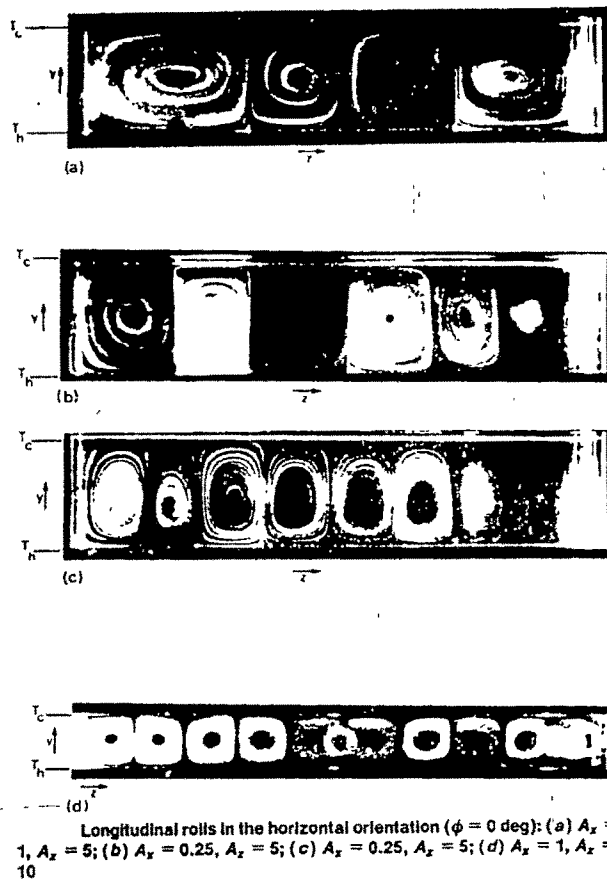


FIG 5-17

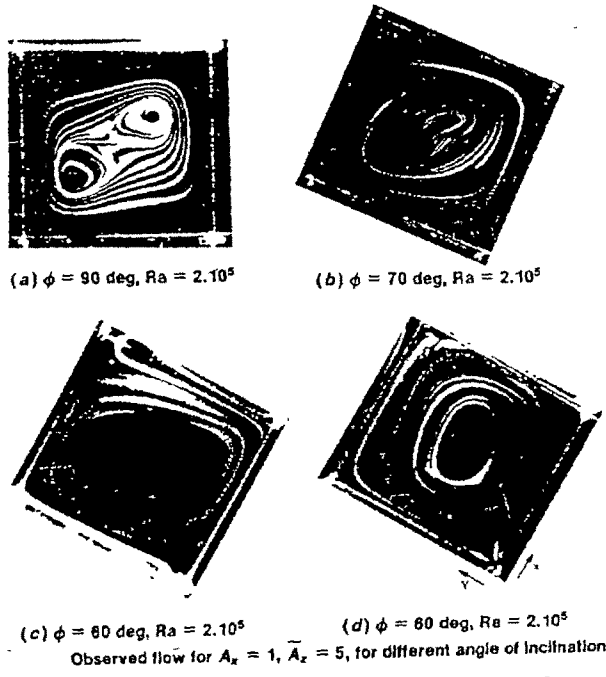


FIG 5-18

Natural convection heat transfer measurements in vertical air layers and in inclined air layers, under top heavy situation, were reported by Elsherbiny et al⁵⁹ in 1982. They varied aspect ratio from 5 to 110, Rayleigh number from 10^2 to 2×10^7 and inclination from 0° to 90° with reference to horizontal.

Their results for vertical layers are shown in Fig.5.19, indicating a complex nature of relationship between Nusselt number and aspect ratio. For inclined layers, they reported the results for $\phi = 60^\circ$ as shown in Fig.5.20. This shows that Nusselt number is aspect ratio dependent for low modified Ra values ($500 < Ra \cos \phi < 2 \times 10^4$) while it is independent of aspect ratio for higher $Ra \cos \phi$ values. Classical critical Rayleigh number $(Ra \cos \phi)_{crit}$ of 1708 was observed to be confirmed for $AR \geq 20$, by them. They also observed that Nu values are independent of inclination ϕ only at low Ra values and that too for near vertical layers only where $60^\circ \leq \phi \leq 90^\circ$.

Effect of inclination on natural convection heat transfer and fluid flow is very well represented in a paper by Symons and Peck⁶³ in 1984, who performed extensive experiments on longitudinal slots of AR from 6 to 12 and on a transverse slot of aspect ratio 6, for inclinations from 0° to 90° and for $Ra < 10^7$. Fig.5.21 and 5.22 represent their results, indicating an existence of high Nusselt number region (for $0^\circ \leq \phi \leq 15^\circ$) and low Nusselt number region (for $25^\circ \leq \phi \leq 90^\circ$), separated by a transition region beginning at $\phi = 15^\circ$ and ending at $\phi = 25^\circ$, for longitudinal slots. They also observed instability (i.e. unstable behaviour of Nusselt number) in the range of inclinations $0^\circ < \phi < 30^\circ$.

Flow visualisation experiments by introducing cigar smoke in the slots, were also performed, the results of which are summarised in Fig.5.23 and 5.24.

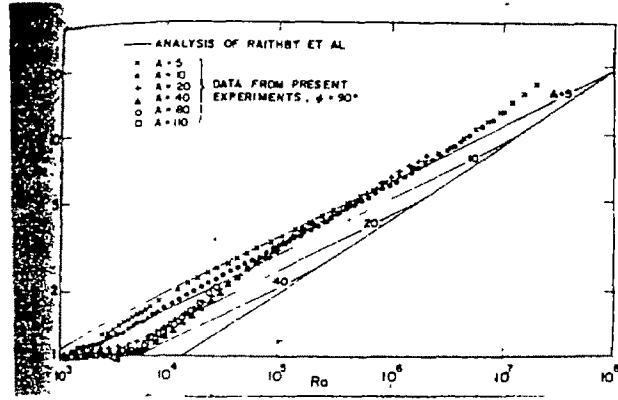


FIG 5-19

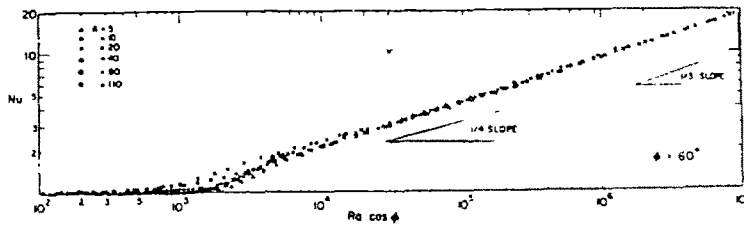


FIG 5-20

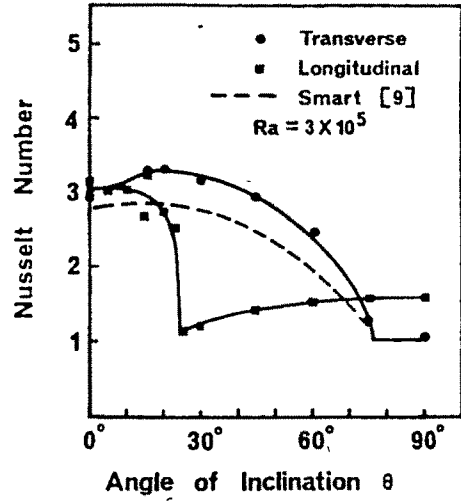


FIG 5-21

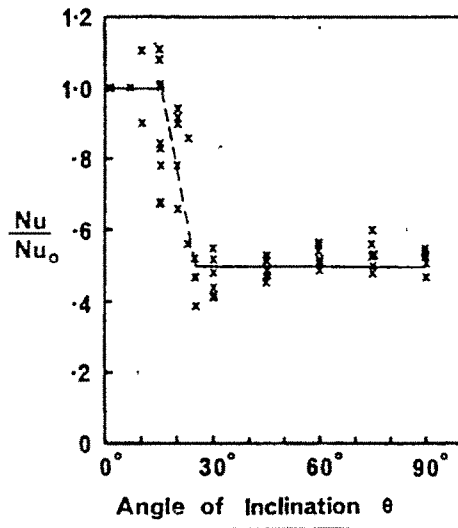
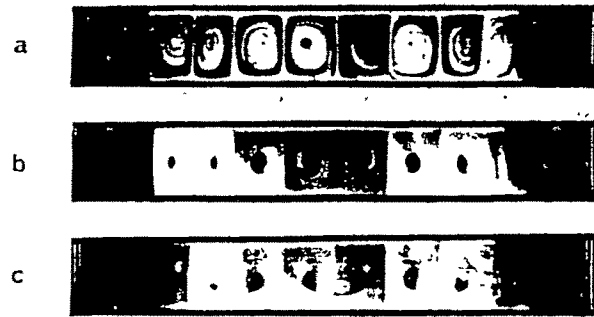


FIG 5-22

Fig.5.23 represents convective flow patterns for a transverse slot at various inclinations. Multicellular convective flow was observed for inclinations upto 70° while a single roll circulation (i.e. uni-cellular flow) was established with a transverse axis for inclinations over 70° , which could not be photographed.

Flow patterns for a longitudinal slot at various inclinations, were similarly documented in Fig.5.24. Multicellular flow with the fluid in consecutive cells rotating in opposite sense, was observed for horizontal, longitudinal slot, the behaviour being comparable to that for horizontal, transverse slot. As the inclination was increased, however, every second cell (those flowing down the hot surface and up the cold surface), became narrower, while the remaining cells became wider. Further increase in inclination resulted in progressive displacement of narrower cells, leaving the wider cells to coalesce. At inclinations beyond 35° with reference to horizontal, all the narrower cells disappeared, converting coalescing wider cells into one long unicell flowing up the hot surface and down the cold surface. This unicell flow structure persisted for all inclinations from 35° to 90° with reference to horizontal.

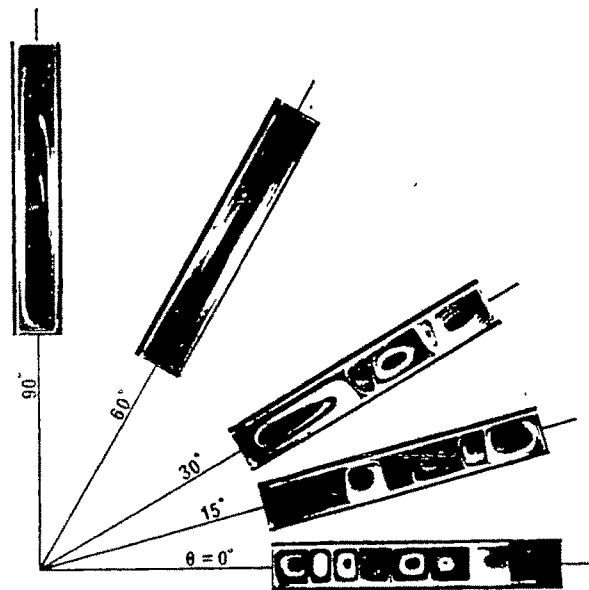
Foregoing survey confirms the inadequacy of any numerical algorithm that has been tried so far, for obtaining a satisfactory solution in case of inclined enclosures, under top heavy arrangement. Experimental findings of earlier investigators suggests the appearance of first criticality at an angle of 15° (5° observed in our case) and that of second criticality at 25° (15° in our case). Aspect ratio dependency in case of inclined enclosures, was not ascertained by earlier investigators, while we have tried to investigate the same, however, we were only partially successful, possibly due to an inadequacy



Convective flow photographs for the transverse slot, $Ra = 3 \times 10^5$, $A = 6$, $H = 60$ mm.

- (a) $\theta = 0$ deg
- (b) $\theta = 30$ deg
- (c) $\theta = 60$ deg

FIG 5-23



Convective flow photographs for the longitudinal slot, for $Ra = 3 \times 10^5$, $A = 6$, $H = 60$ mm, and θ as shown

FIG 5-24

of the computational algorithm used.

Fig.5.25 shows the results for horizontal enclosures heated from above, in which heat transfer is conduction dominated. It indicates an interesting departure from classical conduction behaviour into aspect ratio dependent cellular convection at high Ra values for low aspect ratio enclosures. A further study in this regime may result in revealing conclusions.

A look at the literature survey made earlier, reveals that earlier investigators either ignored the effect of aspect ratio^{44,56} or maintained constant aspect ratio^{61,68} in their investigations. Those who considered the effect of aspect ratio, either studied vertical⁶⁴ or near vertical⁵⁹ enclosures. Arnold et al⁴⁹ varied aspect ratio from 0.2 to 20 in their experimental study on inclined enclosures and found that a further theoretical work is needed due to complex behaviour of fluid at $\phi < 90^\circ$.

Linthorst et al⁵⁸ included aspect ratios from 1 to 7 in their experimental study and suspected the presence of three-dimensional flow. Strada and Heinrich⁶⁰ considered three aspect ratios (1,5 and 10) in their numerical study and found that degree of difficulty in obtaining a solution increases with increase in aspect ratio. None of the above investigators presented any correlation that included an effect of aspect ratio.

Thus, it is difficult to compare our results with the results of earlier investigators, due to non-availability of such results for comparison. However, a crude comparison is made here in TABLE 5.1, from the available results.

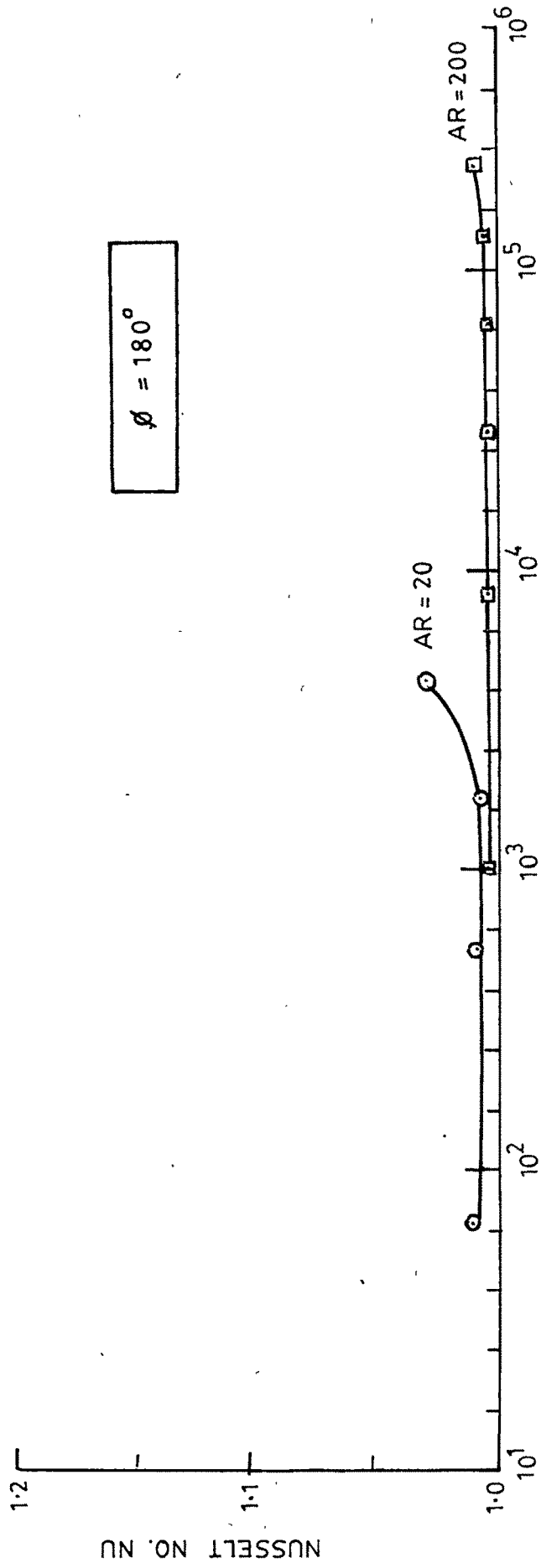


FIG: 5.25

TABLE 5.1
COMPARISON OF RESULTS

Sr.No.	1	2
AR	9.25	1
Ra	3000	10^4
Nu-Buchberg et al ⁴⁴	1.5377	2.1672
Nu-Goldstein et al ¹⁰³	1.4000	-
Nu-Zhong et al ⁶⁸	-	2.4000
Nu-Present	1.122	2.7542

This shows that present results fall below those of earlier investigators at AR=9.25 and rise above those of earlier investigators at AR=1.

A close look at eqn. (5.1) shows that it can be manipulated to make it dimensional one where number of variables reduces to three e.g. critical gap height (H_c) absorber temperature (T_s) and aspect ratio (AR) with cover glass plate temperature (T_1) as a parameter, for solar collector application. Fig. 5.26 is obtained by carrying out such manipulation. This shows that onset of cellular convection from pure conduction in the air gap, depends upon surface temperatures and aspect ratio. It is observed that the curves tend to flatten out showing

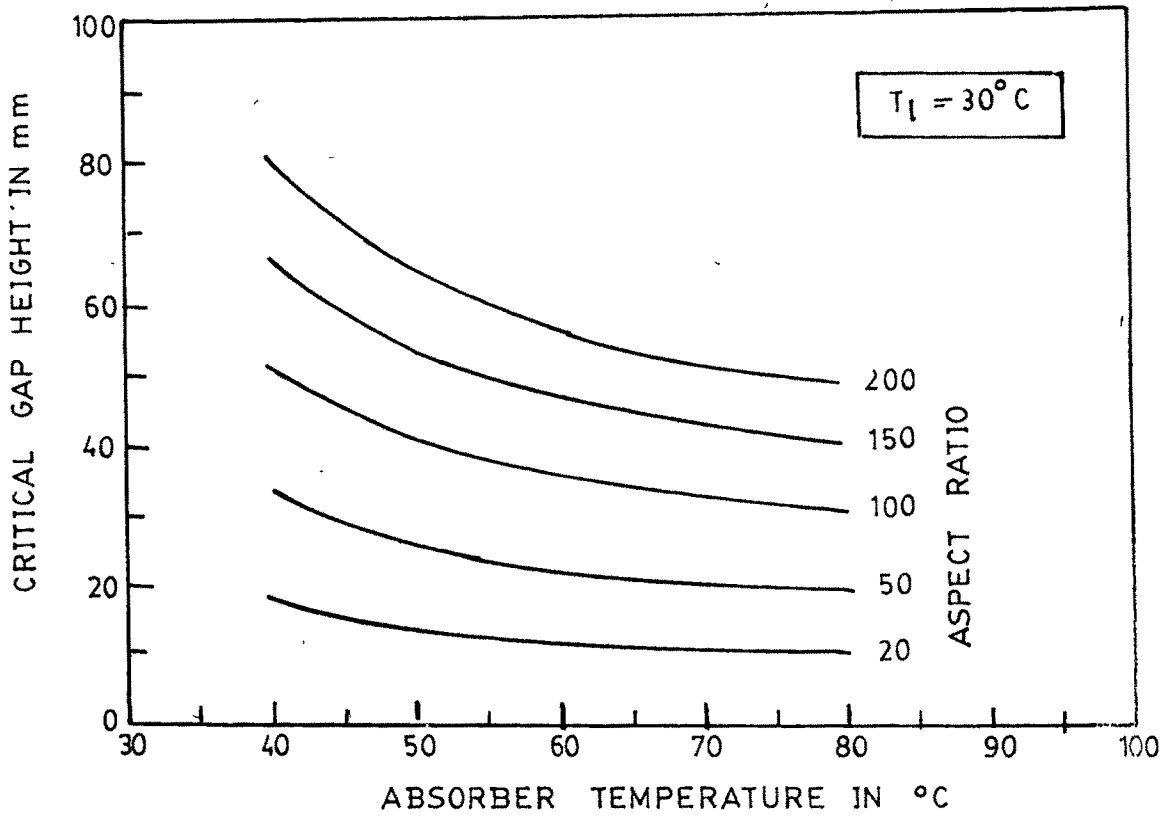


FIG: 5-26

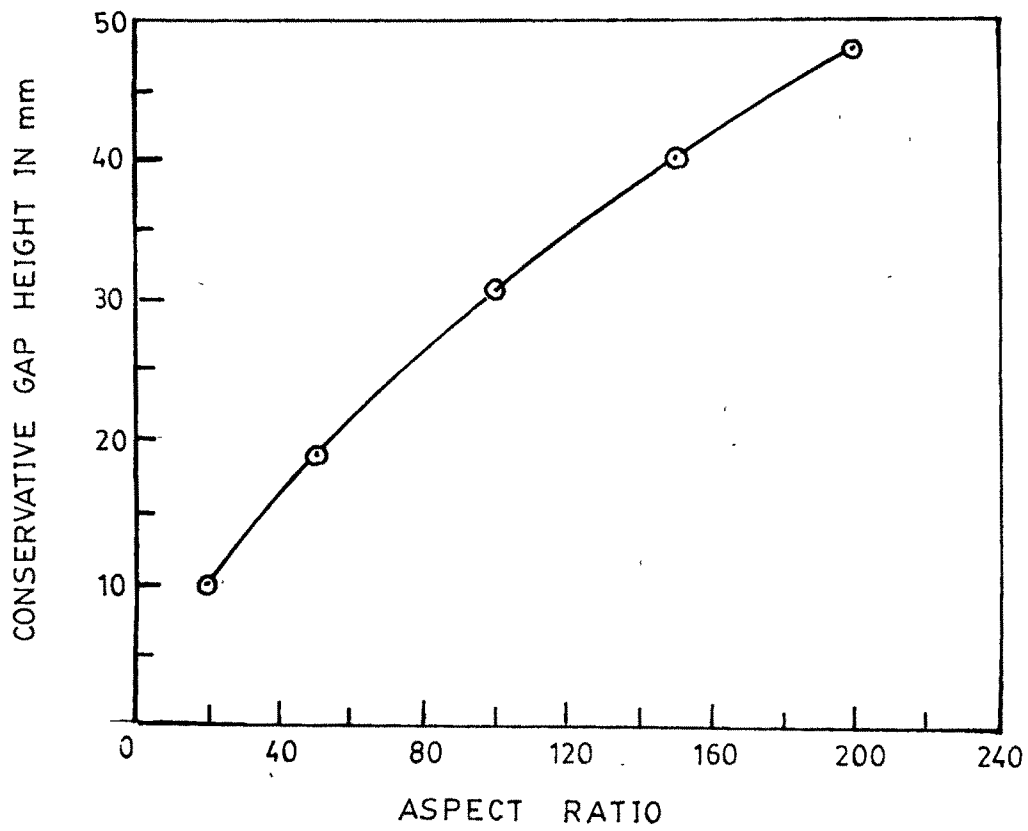


FIG: 5-27

bottom values for critical air gap height at all aspect ratios, below which pure conduction prevails at any surface temperature. This bottom value, coined as conservative gap height, is only a function of aspect ratio, as shown in Fig.5.27.

Use of Fig.5.27 at design stage for selecting the gap height for a desired aspect ratio, ensures that, at all surface temperatures, both of absorber and glass cover plate, in so far as the actual air gap height does not exceed conservative gap height, the losses in the air gap shall be only by pure conduction, which is, of course, unavoidable for unevacuated collectors.